Analysis of the Influence of Angle of Attack on Airfoil Lift: A Computational Study

Avighna Daruka, Mr. Gyaneshwaran Gomathinayagam*

The Doon School Dehradun, Mall Road, India, 248001

April 2024

1 Abstract

The angle of attack of an airfoil determines the amount of lift the airfoil can generate, measuring this effect to maximize the aerodynamic potential of a NACA2412 [National Advisory Committee for Aeronautics] and NACA0010-35 airfoil has been undertaken in this article. This article attempts to bridge the gap by providing a relationship between the angle of attack and airflow-related parameters by undertaking an intuitive computation. Initially, it measures the lift, lift-to-drag ratio, and angle of attack (AOA). The open-source NASA [National Aeronautics and Space Agency] Glenn software manipulates environmental parameters, making research more accessible and eliminating human error. The article summarises that the stall point – where a rapid decrease in lift is seen to decrease the lift coefficient rapidly. Based on the current scientific development in the field, the optimal angle of attack is roughly 0.065 radians for most avionic systems. The lift coefficient increases in a linear relationship with the angle of attack but after a critical point, the lift coefficient rapidly decreases leading to an induced stall, something which has been the root cause for aviation accidents. Furthermore, towards the end of the article, the Bernoulli theorem was derived and proved to demonstrate how fundamental flow dynamics dictate the flight of an aviation object. Using pressure and velocity variation graphs extracted from the NASA Glen open-source software, and comparing the slopes of a set point the article was able to justify the theoretical hypothesis. By understanding the effect of the angle of attack on the lift, one can gain a better understanding of why aviation stalls occur and how they are inherently linked to the rise in the angle of attack. This can lead to aircraft safety and general avionic development in research.

2 Introductory Research and Key Terms

Aerospace research is rapidly developing new technologies for improving aircraft performance and aerodynamics. Developing innovative technology to improve aerodynamic performance will undoubtedly improve commercial aircraft's efficiency, power, and operating costs in the foreseeable future. This article aims to contribute to this research by looking into the fundamental notion of the angle of attack and its link with the lift and drag coefficients, as well as calculating the ratios between these variables. After calculating these variables, graphing and visualizing the relationship will help an understanding of how they are interconnected be established. Furthermore, understanding the basics of fluid mechanics with lift's relation with angle of attack is extremely important as the relationship between angle of attack and lift is critical for anybody involved in aviation, including pilots and engineers.

1. Firstly for controlling flight, pilots may generate more lift for take-off and rising while producing less lift for descent and landing. This provides exact control over the aircraft's flight path. Something that can be established with an understanding of the relationship between lift and angle of attack.

2. Safe flight operations: Understanding this relationship assists pilots in avoiding a stall. A stall happens when the angle of attack becomes too high, disrupting airflow over the wings, and causing a rapid decrease in lift. This phenomenon has been deeply analyzed in the continuation of the article. Starting off, airflow over an airfoil can be divided into laminar and turbulent. In experimental conditions using computational fluid dynamics, the article has simulated laminar flow, as drawing data about turbulent flow is highly inaccurate and unpredictable. However, as airfoil design methodologies mature, it becomes more difficult to obtain optimal aerodynamic performance enhancement merely through shape design. Prospects for aerodynamic research include active flow control, in which aerodynamic performance is not directly tied to airfoil shape but rather using analogue flow control systems. Although this is not mentioned in the paper, prospects can be used to appreciate its advantages over traditional physical flow alteration approaches.

Current studies employ extremely complicated and cumbersome methods to extrapolate data regarding the amount of lift generated by an airfoil. A paper conducted at the National Institute of Science (Ref 4.) employed a Co-Flow Jet (CFJ) technique using complex algorithms to measure the lift. This paper uses a JavaScript 2D flow modeller to measure the lift. This type of methodology has not been conducted yet in regards to measuring flow, and hence it becomes vital to understand basic flow mechanics and aerospace engineering.

In this article, the computational simulation approach initially includes the manipulation of the standard NACA2412 airfoil in software. An uncambered NACA0010-35 airfoil was also under study to investigate the effect of maximum

camber on the stalling point and lift coefficient. After adjusting the environment parameters, one can calculate the drag as well. These models have been modelled in scale representation and then put into the NASA Glenn flow simulator.

The standard nomenclature of terms has been laid out after the references; the article utilizes the following key terms:
Pressure Gradient: Describes the direction and rate at which pressure increases the most rapidly around the airfoil being studied.

Lift: counteracting force to weight and gravity caused by a pressure difference in the airfoil.

Airfoil: A lift-generating surface that is the main contact object with the air.

Laminar Flow: The motion of a fluid where every particle in the fluid follows the same path as its previous particles and is in an orderly structure.

Turbulent Flow: Flow in which the fluid undergoes irregular fluctuations or mixing. Normally diffusive in nature.

Active Flow Control: Installing fluid-managing actuators that help manipulate airflow around an airfoil.

Airfoil thickness: the distance between the upper and lower surfaces of an airfoil at its thickest point.

Fluid viscosity: a measure of a fluid's resistance to flow. Utilized in the Reynolds equation.

Boundary layer: the thin layer of fluid that adheres to the surface of an object moving through a fluid.

Camber: The curvature of an airfoil's surface. An airfoil with positive camber has a curved upper surface, while an airfoil with negative camber has a curved lower surface. Camber can also be defined as when the camber line is not overlapping or the same as the chord line.

Freestream velocity: the velocity of the fluid undisturbed by the presence of an object.

Symmetric or Uncambered Airfoil: Upper and lower surfaces are mirror images, which leads to the camber line being collinear and overlapping with the chord line. A symmetric airfoil will also have a just camber of zero.

Cambered Airfoil: An asymmetric airfoil for which the mean camber line will be above the chord line.

Stall point: The stalling point is defined as the position at which a rapid decrease in lift is noticed.

Below are the diagrams for the airfoils that have been mentioned before. These are the two airfoils that will be studied for today's article. The figure describes certain defining characteristics of an airfoil using an intuitive illustration:

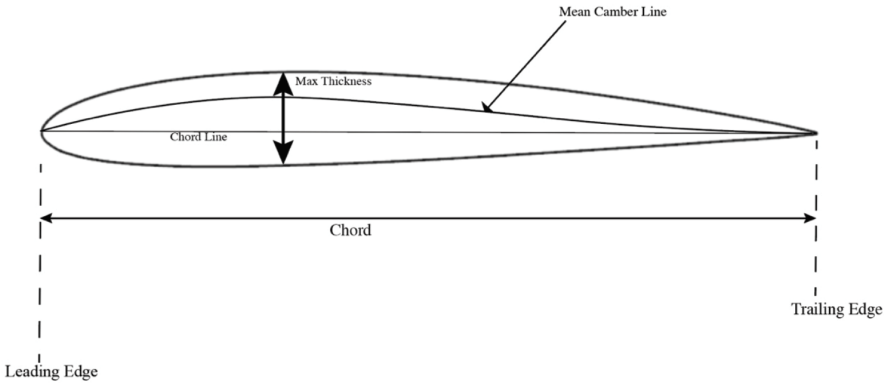

Figure 1: Property Layout

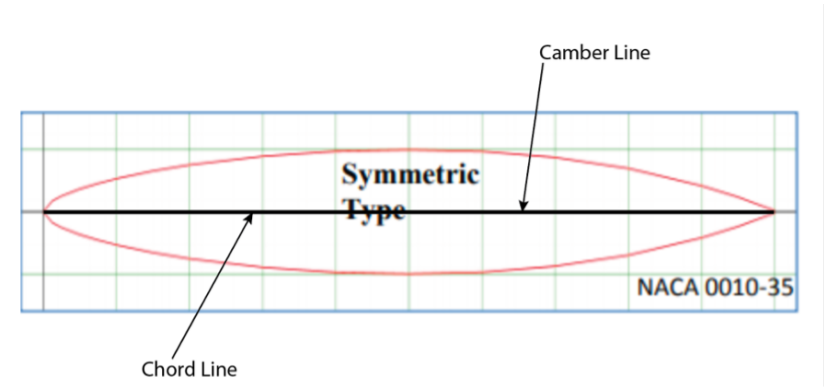

Figure 2: NACA0010-35, Illustration by UIUC Airfoil Database

This diagram is the overall defining characteristics of an airfoil.
Figure 3 describes all the main characteristics that differentiate the two different types of Airfoil that are under discussion. Although this figure has no direct implication in the paper, it is crucial to understand what differences in the airfoil structure mean and how they truly affect the lift produced.

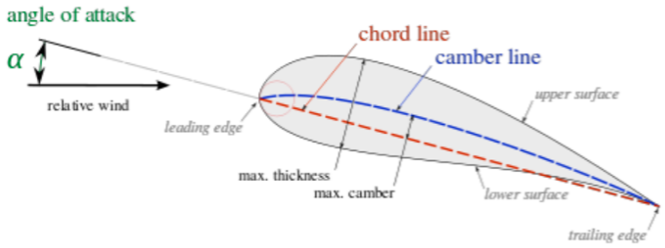

Figure 3: Defining Characteristics

3 Governing Equations

For the research, calculating the lift and drag coefficient to accurately take into consideration all the environmental parameters is needed, this makes the data more accurate and reduces overall uncertainty. Data calculated from these equations has not been illustrated in the tables as they are not relevant to the ongoing investigation.

Below are these equations.
The lift coefficient of an airfoil can be derived from the standard lift equation of an airfoil. (2)

$$C_l = \frac{2L}{\rho A\, v^2} \tag{1}$$

Where:
L - Lift
A – Related surface area
V – Fluid Velocity
The rest of the utilized nomenclature has been mentioned in the Nomenclature section of the article.

4 Computation and Methodology

The software allowed me to alter environment parameters, I took the values according to the average atmospheric conditions at 37500ft.

For data processing, I utilized the NASA Glen Centre of Research JavaScript simulator to vary various parameters. The software was extremely intuitive and easy to understand. Below given is the native environment of the software, and how the airflow has been simulated over the airfoil. Furthermore, I added airflow settings such that it can be understood how the airflow dynamics work. The software worked by allowing me to simulate a native environment where I used a slider to slowly vary the angle of attack. The software then kept all other components and factors constant and gave me the value of the lift. No

Environment Parameters		Miscellaneous Parameters	
Altitude	11430m	Camber	0 - 12%
Initial Freestream Velocity	241.723km/h	Chord Area	5.1ft – Span 20ft.
Relative Humidity	0%	Surface Area	102 sq. ft
		Pressure	14.694 lb/sq. in.
		Density	0.002378 slug / cu ft
		Temperature	59 F.

Figure 4: Environmental Factors (Imported Table)

X – Y coordinates were inputted from the user and during data collection no new JavaScript code was written. Furthermore, the software proved extremely simple to use as only camber percentage and other proprietary properties of the airfoil were needed. Free stream air velocity and constant and other parameters have been mentioned in the table.

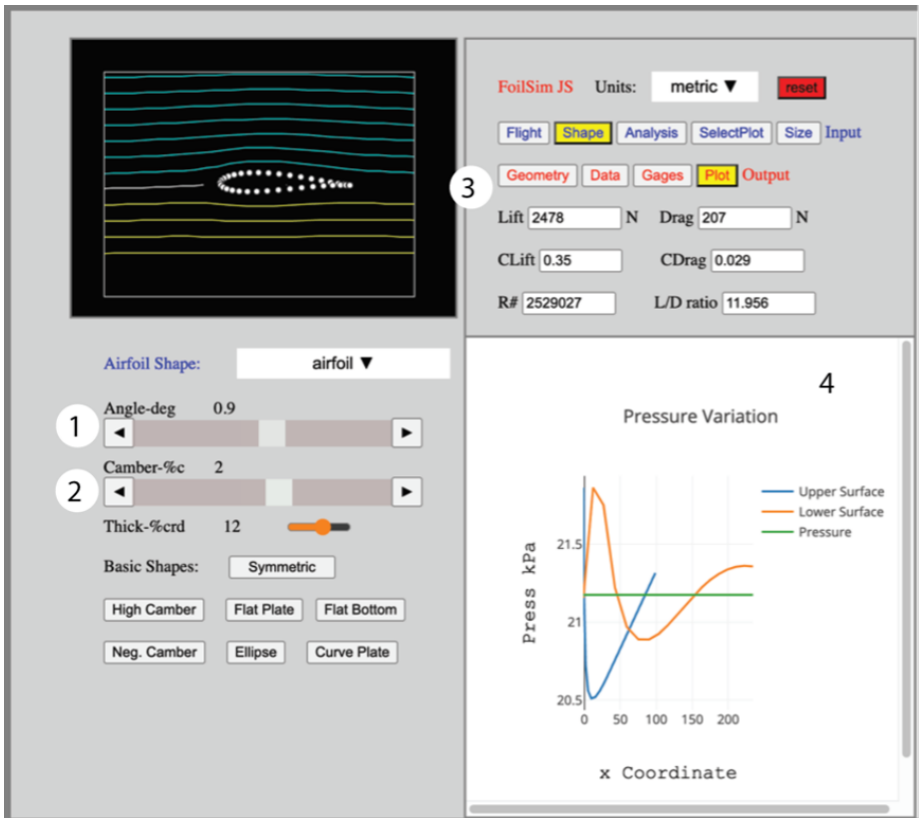

Figure 5: Native Environment

1- Where I altered the angle of attack
2- Where the parameters for the NACA2412 airfoil were inputted
3- Where I received the data
4- Where pressure and velocity variation graphs can be seen.

Note: Software parameters were defaulted for 37500ft.

Using the software, I then proceeded to vary the angle of attack slowly, varying the degree by 1 degree, but after reaching the average angle of attack used by commercial airlines I reduced this increment to 0.1 degrees to increase the overall accuracy of the data collected, this is especially important in areas of 14-16 degrees where one would need to calculate the critical angle of attack. Below is the data, the lift and drag coefficient were calculated with the parameters and formula given in the second section of the article.

5 Results

AOA (rad)	Lift (N)	Drag(N)	L/D Ratio
0	1775	160.1	11.104
0.017	2602	218.0	11.884
0.035	3430	298.0	11.525
0.052	4239	391.4	10.789
0.054	4319	404.8	10.708
0.056	4399	413.7	10.628
0.058	4479	422.6	10.547
0.059	4559	435.9	10.465
0.061	4635	444.8	10.384
0.063	4715	458.2	10.303
0.065	4795	467.1	10.221
0.066	4875	480.4	10.140
0.068	4951	493.8	10.060
0.070	5018	502.6	9.979
0.087	5792	627.2	9.203
0.10	6552	769.5	8.494
0.12	7295	929.7	7.854
0.14	8025	1103	7.278
0.16	8741	1294	6.760
0.175	9439	1499	6.293
0.192	10080	1713	5.884
0.209	10610	1913	5.540
0.227	11000	2095	5.250
0.244	11250	2246	5.006
0.262	11330	2362	4.799
0.279	11240	2433	4.622
0.297	10940	2451	4.467
0.314	10420	2411	4.323
0.332	9644	2313	4.173
0.349	8585	2153	3.986
Average	**6991**	**1130**	**-**

Figure 6: Data for Cambered Airfoil

Using the data I plotted my results on a graph utilizing the logger pro software.

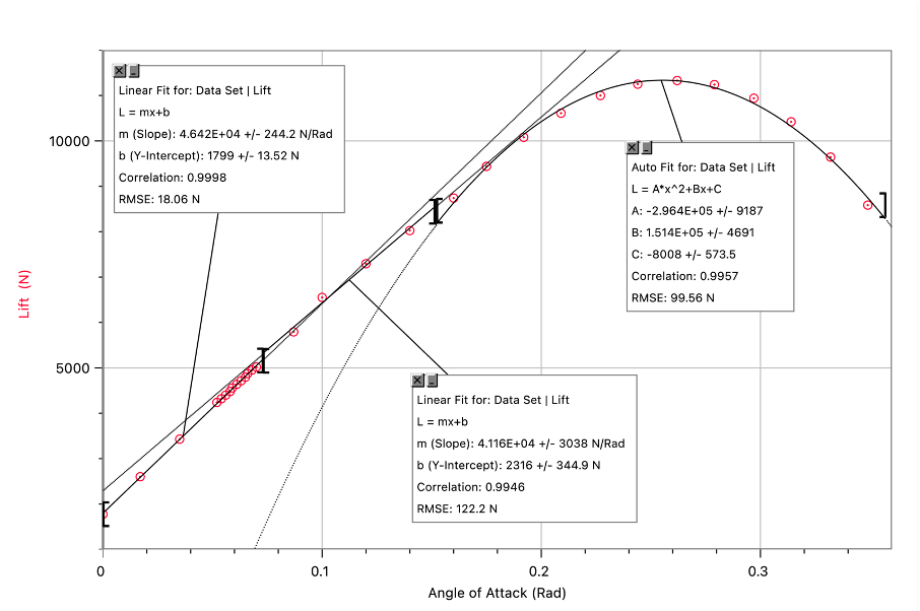

Figure 7: Cambered Airfoil Data Plot

Now that the data is collected, understanding the stall point becomes important. This is critical for understanding the basic flow dynamics of a cambered airfoil. While looking for the stall point, one must investigate the location where the quantity of lift suddenly and dramatically decreases. To do this intuitively, I plotted lift against angle of attack to visualize the cambered airfoil's flow dynamics. This is seen in 7.

According to figure 7 understanding the stalling point of the NACA2412 airfoil becomes easy. When representing it one can estimate the airfoil to have a stalling point of roughly 0.258 radians.

Now to compare it with the uncambered airfoil, one would need to keep all other factors other than the camber percentage constant. The speed, altitude and all other environmental parameters were kept consistent to improve overall accuracy. The camber percentage was 0 per cent with all other parameters remaining the same. The max chord thickness remained at 12 per cent.

AOA(rad)	Lift (N)	Drag(N)	L/D Ratio
0.017	872	138	6.262
0.035	1731	173	9.920
0.052	2567	227	11.373
0.054	2651	231	11.434
0.056	2736	240	11.484
0.058	2816	245	11.522
0.059	2901	249	11.551
0.061	2981	258	11.570
0.063	3065	262	11.581
0.065	3145	271	11.583
0.066	3230	280	11.578
0.068	3310	285	11.566
0.070	3390	294	11.548
0.087	4200	378	11.107
0.105	4992	480	10.405
0.122	5766	601	9.619
0.140	6526	738	8.832
0.157	7269	899	8.081
0.175	7999	1081	7.385
0.192	8675	1281	6.767
0.209	9245	1481	6.237
0.227	9694	1677	5.783
0.244	11000	1855	5.393
0.246	10030	1873	5.357
0.248	10050	1886	5.322
0.250	10070	1904	5.287
0.251	10090	1922	5.252
0.253	10100	1935	5.218
0.255	10120	1953	5.185
0.257	10130	1966	5.152
0.258	10140	1979	5.119
0.260	10150	1997	5.087
0.262	10160	2011	5.055
0.279	10140	2131	4.461
0.297	9930	2206	4.499
0.314	9503	2233	4.259
0.332	8831	2193	4.028
0.349	7888	2086	3.782
Average	**6792**	**1155**	**-**

Figure 8: Uncambered Airfoil data

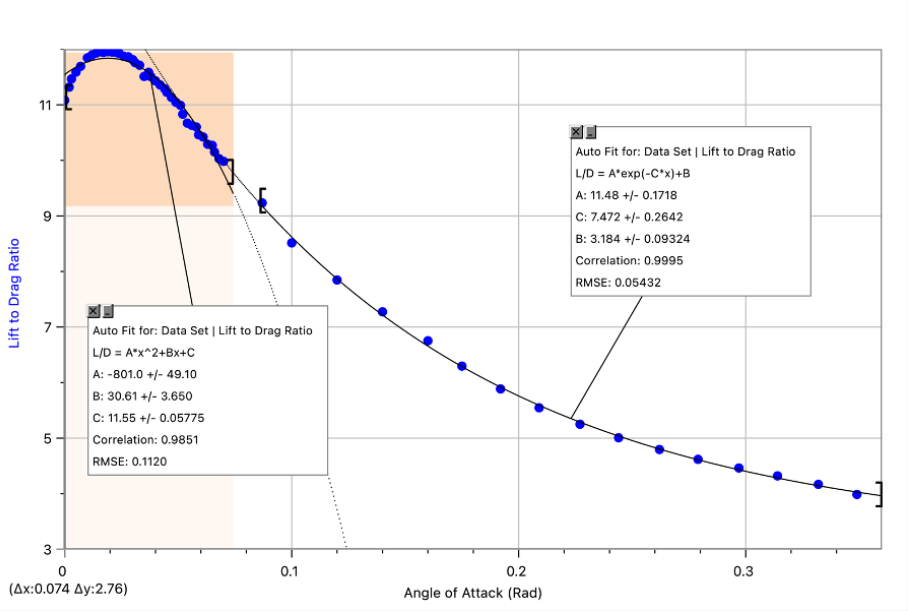

Figure 9: Relation between L/D ratio and AOA

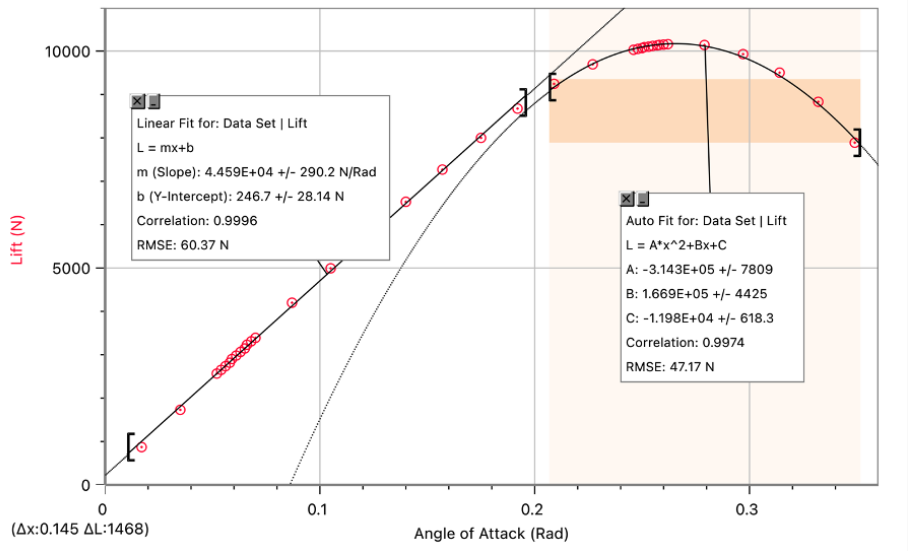

Figure 10: Uncambered Airfoil Data Plot

For the uncambered airfoil, I have plotted the lift with respect to the angle of attack, as seen in Figure 10. But a plot has also been constructed in Figure 9 regarding the L/D ratio and angle of attack, something that will be looked over later in the article.

A similar exponential relationship in the beginning can be seen, but after roughly 0.337 radians the drag coefficient also decreases.

Extrapolating the results, the uncambered airfoil has a stalling point of around 0.267 radians. When the data is compared, the uncambered airfoil has a higher stall point, but lower average lift and higher average drag. For commercial aircraft operating at an angle of attack of approximately 0.559 radians during take-off, a cambered airfoil is the preferable choice due to its high aerodynamic efficiency.

6 Data Analysis and Discussion

When varying the angle of attack, one can observe an initial linear relationship between the angle of attack and lift. However, after a critical point, the point of linearity is defined as the critical angle of attack. A decrease in the coefficient of drag at an angle of 0.349 radians is likely due to changes in pressure distribution and boundary layer behaviour around the object. At lower angles of attack, the flow may separate from the surface earlier, leading to increased drag. However, as the angle of attack increases, the pressure distribution changes, often resulting in the flow remaining attached to the surface for longer periods. Flow separation leads to induced drag as it generates a low-pressure zone behind the object, pulling it backwards. Furthermore, turbulent eddies result in energy loss and pressure imbalances, which contribute to drag.

6.1 Phenomenon Explanation

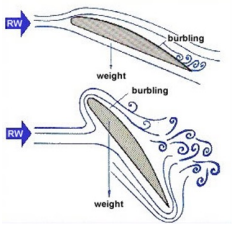

Figure 11: Representation of Stall

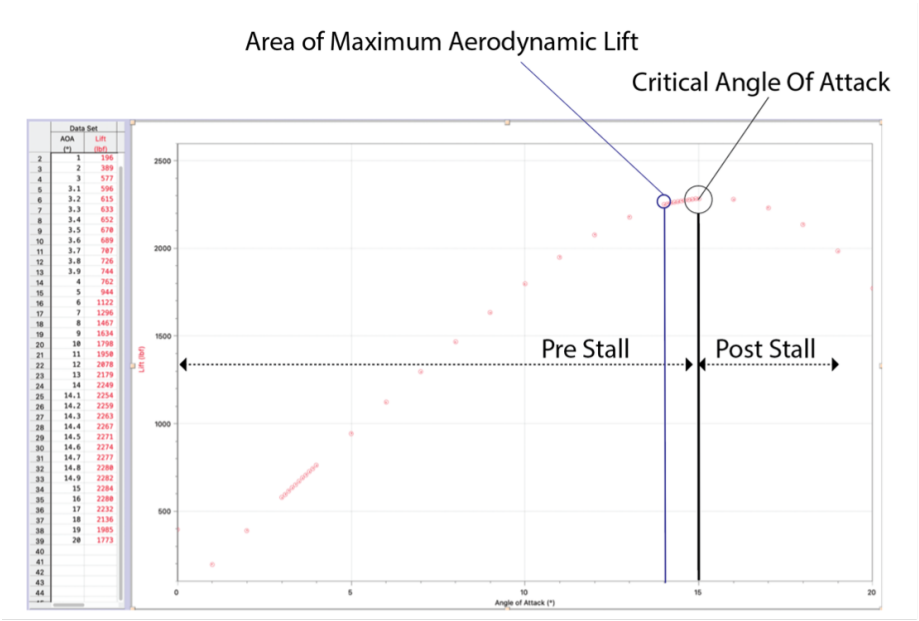

Figure 12: Stall Derivation

Beyond the critical angle of attack, airflow separates, resulting in turbulent eddies and a reduction in lift. This gap alters the pressure distribution over the wing, exacerbating the loss of lift. Furthermore, airspeed, weight distribution, and wing design all have a substantial influence on stall behaviour.

6.2 Principle Proof of Bernoulli's theorem

Another parameter that has been investigated is the pressure variation with respect to the velocity, this is governed by Bernoulli's theorem which states that an area of airflow travelling at a higher velocity will experience a region of less pressure.

This section aims to derive this theory by calculating the positive and negative gradients of the airflow in pressure and velocity variation graphs. Simulations were run on average Earth's atmosphere. Below are the graphs extrapolated from the data collection.

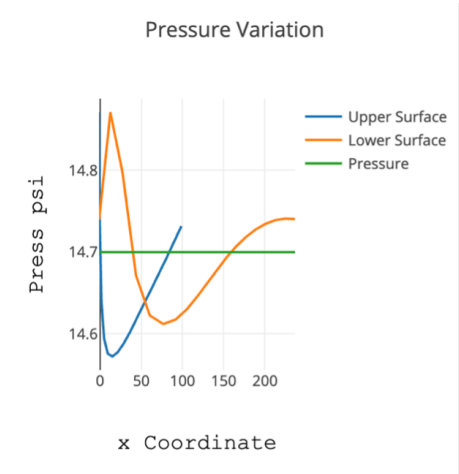

Figure 13: Pressure Variation

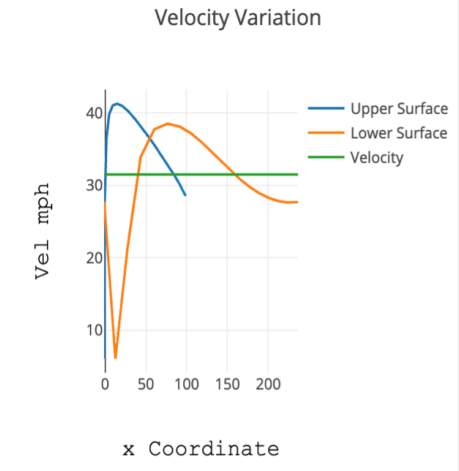

Figure 14: Velocity Variation

Using the standard equation of slope:

$$m = \frac{\Delta y}{\Delta x} \tag{2}$$

Slope of pressure variation graph [Lower Surface]:

$$m = \frac{14.71698 - 14.70395}{12.48166 - 0} \tag{3}$$

$$m = 0.00104393 \tag{4}$$

Slope of the velocity variation graph [Lower Surface]:

$$m = \frac{6.046926 - 0}{12.48166 - (-0.4374458)} \tag{5}$$

$$m = 0.486060 \tag{6}$$

Hence proved how the velocity is affected by the pressure in a non-proportional manner as the two slopes of the graphs calculated have unequal slope calculations.

6.3 Limitations

The article contains a lot of limitations that lead to inaccuracy in the data being collected.

1. The average values for the coefficient of drag were only taken up to 4-6 significant figures which leads to experimental accuracy in the comparison of cambered and uncambered airfoils. This problem could be solved when taking larger numbers with greater decimal accuracy. However, since the difference in coefficient of drag in cambered and uncambered airfoils is already quite significant in magnitude this limitation does not affect the visual comparison.

2. Experimental inaccuracy in the slope calculation for proving the basic Bernoulli principle is extremely plausible as the coordinate points were extremely unreliable on the JavaScript software. The point used to calculate the slope of the velocity variation could have very well be inaccurate. Unfortunately, due to technical limitations, I could not plot more accurate data.

3. Taking a simulation-based investigation allowed the degree of human error to be limited. Since this computational approach could have its own coding errors which I am not aware of leading to an error of an unknown magnitude.

7 Conclusion and Further Prospects

As per the results of the trials understanding the concrete effect of the angle of attack on the lift generated becomes simple. According to the data collected the linearity between the AOA and lift was only up to the critical angle of attack, after which the lift rapidly decreased leading to an induced stall.

My basic proof of Bernoulli's principle shows the effect of airflow speed on pressure, errors in the basic proof could be shown to also point out errors in the slope calculation. My display in the basic differences of a cambered and uncambered airfoil also shows the effect of camber on aerodynamic performance and how airfoils that are employed in the wings of today's aircraft have been optimized to make lift and other factors the most efficient.

The Reynolds number of the fluid flow was not defined in the article leading to a less experimental effect on the day-to-day practicality of the article. The drag coefficient was also investigated to measure the relationship between lift and drag coefficient to show how it is not always a linear relationship and how the drag coefficient can also decrease with respect to the angle of attack.

The optimum angle of attack was investigated to be around 1 degree for the NACA-2412 airfoil. In comparison to a paper published by Venkatesan, S, Kumar, P., Kumar, S, and Kumar, S; this value does fall very close in accordance with their calculated value of 1 degree as well. This proves how with a simpler and more intuitive computational simulation, one can get the same reliable results.

The hypothesis-driven research was extremely productive, the article successfully proved the dangerous effects of an induced stall on the rapid decrease in the amount of lift. Along with this, the proof of Bernoulli's principle displayed how aircraft can fundamentally produce lift in the first place. I hope this article was able to provide a description of fundamental fluid mechanics and illustrate the effect of the angle of attack on the lift produced. I mostly employed the usage of diagrams because this topic can be easily described in an intuitive manner using illustrations and diagrams since airflow is a topic that can be intricate and hence this article aims to explain complicated topics while investigating a very fundamental concept in an intuitive manner and respect.

From the graph plotted, the maximum lift-to-drag ratio is at 0.019 radians, but the lift force over here is only 24 per cent that of the maximum lift achieved at 0.262 radians, and hence the most efficient area doesn't mean the most useful. A stronger engine would be required to push commercial airlines.

Further research could be conducted to measure the pressure gradient of the airfoil to investigate a lot more parameters. This research could be implemented to further investigate the ideal airfoil shape and how the NACA2412 airfoil could be modified to make the aerodynamic properties of the airfoil the most efficient and optimized for fairflow in the desired conditions.

8 References

1. Katz, J., & Plotkin, A. (1991). Low-Speed Aerodynamics (01, Ed. Vol. 01). Mc-Graw Hill, Inc.

2. Shinde, M. S., Shinde, V., Shirode, S., & Shriwas, D. (2021). Simulation of Flow over Airfoil. International Research Journal of Engineering and Technology (IRJET), 08(04), 11,12,13,14,15,16,17.

3. Venkatesan, S., Kumar, P., Kumar, S., & Kumar, S. (2018). Computa-

tional analysis of aerodynamic characteristics of dimple airfoil naca 2412 at various angles of attack. International Journal of Mechanical Engineering and Technology (IJMET), 8(9), 41-49.

4. Wang, R., Zhang, G., Ying, P., & Ma, X. (2022). Effects of Key Parameters on Airfoil Aerodynamics Using Co-Flow Jet Active Flow Control. In. Institute of Engineering Thermophysics, Chinese Academy of Sciences, Beijing 100190, China.

5. Cleynen, O. (2011). Airfoil nomenclature In W. p. nomenclature.svg (Ed.), Wikipedia (Vol. 800 x 399 px): Wikipedia.

6. Database, U. A. f. Geometry for NACA 0010-35 In naca001035.gif (Ed.). Illinois: UIUC.

9 Nomenclature and Acknowledgements

m	Total mass flow rate through actuators
p	Static pressure
Re	Reynolds number based on mean aerodynamic chord
S	Wing reference area
V	Total velocity
3-D	Three-dimensional
X ; Y; Z	Cartesian coordinates
α	Angle of attack
μ	Fluid Viscosity
ρ	Density